HHS Public Access

Author manuscript

Oncogene. Author manuscript; available in PMC 2013 June 13.

Published in final edited form as:

Oncogene. 2012 December 13; 31(50): 5144–5152. doi:10.1038/onc.2012.1.

A proprotein convertase/MMP-14 proteolytic cascade releases a novel 40 kDa vasculostatin from tumor suppressor BAI1

Sarah M. Cork[1], **Balveen Kaur**[1,*], **Narra S. Devi**[1], **Lee Cooper**[2], **Joel H. Saltz**[2,4], **Eric M. Sandberg**[1], **Stefan Kaluz**[1,4], and **Erwin G. Van Meir**[1,3,4,**]

[1]Laboratory of Molecular Neuro-Oncology, Department of Neurosurgery, Emory University School of Medicine, Atlanta, GA

[2]Center for Comprehensive Informatics, Emory University, Atlanta, GA

[3]Department of Hematology and Medical Oncology, Emory University School of Medicine, Atlanta, GA

[4]Winship Cancer Institute, Emory University, Atlanta, GA

Abstract

Brain angiogenesis inhibitor 1 (BAI1), an orphan GPCR-type seven transmembrane receptor, was recently found mutated or silenced in multiple human cancers and can interfere with tumor growth when overexpressed. Yet, little is known about the molecular mechanisms through which this novel tumor suppressor exerts its anti-cancer effects. Here, we demonstrate that the N-terminus of BAI1 is cleaved extracellularly to generate a truncated receptor and a 40 kDa fragment that inhibits angiogenesis. We demonstrate that this novel proteolytic processing event depends on a two-step cascade of protease of activation: proprotein convertases, primarily furin, activate latent matrix metalloproteinase 14, which then directly cleaves BAI1 to release the bioactive fragment. These findings significantly augment our knowledge of BAI1 by showing a novel posttranslational mechanism regulating BAI1 activity through cancer-associated proteases, have important implications for BAI1 function and regulation, and present novel opportunities for therapy of cancer and other vascular diseases.

Introduction

The brain angiogenesis inhibitor 1 (BAI1) receptor is being increasingly recognized as a critical tumor suppressor in human cancer development. BAI1 expression is lost in the formation of several tumor types including brain, colon and gastric cancer and this loss correlates with poor patient survival (1-5). Overexpression of full-length exogenous BAI1,

**To whom correspondence should be addressed:Erwin G Van Meir, PhD, Winship Cancer Institute, Emory University, 1365C Clifton Rd, NE, room C5078, Atlanta, GA 30322, USA, evanmei@emory.edu Office telephone: +1-404-778-5563, Fax: +1-404-778-5550.
*New address: Dardinger Laboratory for Neuro-oncology and Neurosciences, [1]Department of Neurological Surgery, James Comprehensive Cancer Center, The Ohio State University Medical Center, Columbus, OH, 43210

Conflict of interest.
The authors declare they have no competing interests.

either through stable transfection or gene therapy, slows the growth of several cancer types in tumor xenografts (6–8). More recently, somatic mutations of BAI1 and its family members BAI2 and BAI3 have been identified in lung, breast and ovarian cancers (9), and the *BAI1* gene is silenced via epigenetic mechanisms in glioblastoma (10). The precise mechanisms whereby BAI1 exerts its tumor-suppressive activity in the brain and other organs are unknown and need to be urgently established toward therapeutic exploitation.

BAI1 was identified in a screen for p53-regulated genes (11) and its known features were recently reviewed (12). It was initially proposed as a candidate effector for the anti-angiogenic activity of p53 (13), due to its structure (11). BAI1 is classified as an adhesion-type GPCR and is characterized by a long extracellular N-terminus (120 kDa), which includes an integrin-binding Arg-Gly-Asp (RGD) motif, five thrombospondin type 1 repeats (TSRs) and a putative hormone binding site (Figure 1A). BAI2 and 3 are organized similarly, although they have only four TSRs and lack the RGD motif (12). TSRs are found in more than 70 proteins encoded in the human genome, and among the best-understood properties of TSRs is their ability to inhibit angiogenesis (14) via several mechanisms including interference with vascular endothelial growth factor (VEGF)-heparin attachment (15) or engaging the CD36 receptor on endothelial cells via a VTCG motif to initiate apoptosis (16-18). Not all TSRs are anti-angiogenic, and individual TSRs within the same proteins can have divergent structure and function (19). It is therefore important to derive a precise understanding of the role of each TSR in a given protein to define their bioactivity. The TSRs in BAI1 appear to serve different functions, depending on cell type. In full length BAI1, they act as binding motifs for phosphatidylserine on the surface of apoptotic cells and mediate their engulfment by macrophages (20). In glial cells, N-terminal cleavage of BAI1 generates a low abundance 120 kDa fragment containing all five TSRs, which when overexpressed shows anti-tumor and anti-angiogenic activity independent of the parent receptor (21–23).

Here, we present the discovery of a much more abundant, previously unknown N-terminal fragment of BAI1 of approximately 40 kDa, identify its processing mechanism and demonstrate that it is cleaved extracellularly. We have mapped the site of proteolysis and determined that it contains the RGD motif and just the first TSR. We initially hypothesized that this cleavage might be a mechanism to inactivate the N-terminus of BAI1, but unexpectedly, found that this shedded fragment is potently anti-angiogenic *per se*, and thus we have termed it Vasculostatin-40 (Vstat40). These findings advance our understanding of BAI1 as an important regulator of tissue angiostasis through the paracrine release of multiple soluble angiostatic fragments and reveal new avenues for future therapeutic development.

Results

The N-terminus of BAI1 is processed to yield a major 40-kilodalton secreted fragment

In an investigation of BAI1 expression in normal and neoplastic human brain, we discovered a novel BAI1-derived fragment (Figure 1A) approximately 40 kDa in size and immunoreactive with an anti-terminal BAI1 antibody recognizing N-terminal amino acids 103-118 (N-Ab). This fragment and full length BAI1 were reduced or absent in four

randomly chosen glioblastoma (GBM) tissues (Figure 1A) and *BAI1* mRNA expression levels correlated significantly (p=0.034) with patient survival (Figure 1B), suggesting a potential role in antagonizing gliomagenesis. To determine whether this new fragment resulted from cleavage of the parent BAI1, we transfected a BAI1 expression vector in 293 cells and analyzed the CM by Western blot. This experiment evidenced a prominent band approximately 40 kDa in size, representing the major secreted product of BAI1 (Figure 1C). Similar results were obtained in fibroblast and other glioma cell lines (not shown). Upon longer exposure, a 120-kDa fragment (Vstat120) we previously identified (21) was also detected (Figure 1C, long exposure panel). Henceforth, we wished to evaluate the function of the novel 40 kDa secretion product of BAI1.

We first questioned if the 40 kDa fragment was processed independently of Vstat120 or whether the processing of Vstat120 represented an intermediary step in the generation of the 40 kDa fragment. Thus, we transfected 293 cells with a Vstat120 expression vector (Figure 1C, lane 3) and determined that the 40 kDa fragment is processed from Vstat120 albeit at significantly lower efficiency compared with its processing from full-length BAI1, suggesting that the generation of Vstat120 is unlikely to be a required step for production of the 40 kDa fragment. To follow up on this observation, we investigated processing of Vstat120 and the 40 kDa fragment using a BAI1 mutant containing a point mutation in the GPS region ($S_{927}D$). We observed that the mutant yielded increased levels of Vstat120 production and a corresponding decrease in the secretion of the 40 kDa fragment (Figure 1D), suggesting that secretion of Vstat120 interferes with the generation of the 40 kDa fragment. To investigate the role of the C-terminal region of BAI1 in the extracellular processing of BAI1, we generated a truncated form of BAI1 containing its extracellular domain and three transmembrane domains (BAI1-3TM). We observed that this truncation interferes with secretion of both Vstat120 and the 40 kDa fragment (Figure 1E), suggesting that a complete transmembrane domain or the intracellular portion of BAI1 are required for efficient generation of the 40 kDa fragment.

The N-terminal 40-kDa fragment of BAI1 inhibits angiogenesis in culture and *in vivo*

Based upon the location of the epitope used for its detection and its size, we predicted that the 40 kDa fragment might encompass the RGD and the single most distal TSR, of unknown function. To examine whether this fragment might be capable of exerting any effects on angiogenesis, we generated LN229-L16 glioma cells stably expressing the 40 kDa fragment (Vstat40) or Vstat120 fragment as a comparison, and demonstrated their secretion in the CM (Figure 2A). To determine the Vstats' effect on endothelial cell (EC) migration, we used the CM in a Boyden chamber migration assay using CD36+ HDMECs and CD36-deficient HUVECs (23) (Figure 2B). Both Vstats CM significantly inhibited the serum-induced migration of the HDMECs but not the migration of HUVECs. To investigate whether CD36 expression on endothelial cells is necessary for the anti-angiogenic activity of Vstat40, we tested whether an anti-CD36 function-blocking antibody would rescue migration of HDMECs in the presence of Vstat40. The migration of wounded confluent HDMECs was significantly inhibited in the presence of Vstat40 or Vstat120-containing CM versus control medium (Figure 2C). The antibody neutralized the inhibitory effect of the Vstats on EC migration, while an isotypic control antibody had no effect. To determine whether Vstat40

interferes with complex angiogenesis events such as vascular structure formation, we used an endothelial cord formation assay. HDMECs formed tube-like structures when plated on matrigel in control medium, a process inhibited by more than 50% in the presence of Vstat40-CM, with Vstat120-CM exhibiting an even stronger inhibition (Figure 2D). The presence of Vstats in the CM did not have a significant effect on cord or enclosed structure formation of HUVECs plated under the same conditions. Finally, we investigated whether Vstats interfered with biological angiogenesis using a quantitative *in vivo* angiogenesis model (24). We observed that neovascularization of basement membrane extract prepared with Vstat-CM was reduced in comparison to control CM and quantification of fluorescence-associated angiogenesis demonstrated a significant inhibition in Vstat40- or Vstat120-containing angioreactors versus control ($p=0.011$ and 0.008, respectively) (Figure 2E). We conclude that the 40-kDa fragment potently inhibits specific aspects of angiogenesis in culture and *in vivo*, justifying its designation as a novel Vasculostatin (Vstat40).

Identification of the site of Vstat40 processing

Based on the observation that BAI1 N-terminal constructs containing the Vstat40 cleavage site are processed to some extent into true Vstat40 (e.g., Figure 1C), we reasoned that we could narrow down the location of the processing site by examining the cleavage of progressively shorter N-terminal fragments. Accordingly, we generated serial truncations of N-terminal *Bai1* cDNA flanking the region of Vstat40 cleavage based on its predicted size, and transfected cDNA constructs containing these truncations into 293 cells. Processing of the resulting peptides narrowed the location of Vstat40 cleavage to between amino acids 296 and 349 (Figure 3A). Use of Western blot does not permit the distinction of cleaved and uncleaved fragments differing in only a few amino acids' size. To overcome this limitation, we generated expression vectors that added 3 kDa V5/His tags to the uncleaved N-terminal fragments. Using this approach we were able to demonstrate that Vstat40 is processed between amino acids 321 and 329 (Figure 3B). Finally, to determine the relative contribution of selected amino acids within this region to Vstat40 processing, we used an alanine mutation approach to introduce point mutations in the prospective region of cleavage of the full length BAI1 (Figure 3C). The presence of an $SLR_{328} \rightarrow AAA$ mutation completely abrogated BAI1 processing into Vstat40 (compare lanes 2-3), while an $RSQ_{325} \rightarrow AAA$ mutant had little effect. Combined, these data support that the location of Vstat40 processing is in-between amino acids 321 and 329 and that amino acids 326-328 are essential for the cleavage (Figure 3C).

Inhibition of furin activity reduces Vstat40 processing

No canonical cleavage motifs were apparent in the identified proteolysis site, preventing immediate recognition of the identity of the protease cleaving Vstat40 from BAI1. In a screen for candidate enzymes we used a series of protease inhibitors on BAI1-transfected 293 cells and found that treatment with the irreversible proprotein convertase (PCs) inhibitor dec-RVKR-cmk significantly abrogated the release of Vstat40 in the CM in a dose-dependent manner (Figure 4A). Since furin is a major PC, we examined whether furin was involved in Vstat40 generation. Transient expression of BAI1 in human colon adenocarcinoma LoVo cells, which lack furin activity due to two mutated *fur* alleles (25),

yielded reduced processing of Vstat40 compared with that found in the CM of *Bai1* cDNA transfected LN229 cells (Figure 4B). Processing of Vstat40 was largely restored in LoVo cells with stable transfection with wild-type *fur* cDNA. These cells expressed furin levels comparable to those found in LN229 cells and had functional furin as assessed by the level of processing of the known furin target MMP-14 (26) from its pro-peptide (63 kDa) to its active (60 kDa) form (Figure 4C). Together these results suggest that activity of PCs, particularly that of furin, are involved in Vstat40 processing.

To further confirm the association of furin activity and Vstat40 levels, we knocked down furin protein expression with siRNA in U251MG glioma cells stably transfected with a BAI1 expression vector (U251-BAI1) (23). Furin levels were strongly reduced at all time points under consideration (Figure 4D). The secreted (active) form of MMP-2 was used as a positive control for furin activity, as MMP-2 is activated by furin target MMP-14, and is cleaved by furin as well (27). As expected, no cleaved MMP-2 was observed in the CM of cells subjected to furin knockdown while levels of pro-MMP-2 in the whole cell extract (WCE) were relatively unchanged. Vstat40 processing was strongly inhibited 48 hours after furin siRNA transfection, but unexpectedly levels of secreted Vstat40 reverted to baseline 72 hours post-transfection, even though furin levels remained reduced, suggesting involvement of a compensatory mechanism.

Finally, we performed an *in vitro* cleavage experiment to determine whether furin can directly process the extracellular domain of BAI1 into Vstat40 (Figure 4E). We observed that levels of Vstat40 and Vstat120 remained constant after 18.5 hours of incubation (4E, left panel), indicating that furin is not able to directly process Vstat40, which is in agreement with the absence of a canonical PC cleavage sequence (RxxR) in BAI1 (28). Activity of the recombinant furin in these reaction conditions was confirmed by incubation with the fluorogenic substrate peptide Boc-RVRR-AMC (4E, right panel). In sum, these data suggest that proprotein convertase activity is important for Vstat40 processing, but does not directly cleave BAI1. We then considered that PCs may promote Vstat40 cleavage by indirectly activating the enzyme responsible for BAI1 cleavage.

A furin-activated metalloproteinase processes extracellular BAI1 into Vstat40

Furin processes over a hundred known targets into their bioactive forms (29), including multiple subclasses of metalloproteinases, extracellular proteases which often process cell-adhesion molecules and are, therefore, prime candidate molecules to cleave BAI1. Treatment of U251-BAI1 cells with the general metalloproteinase inhibitor GM6001 inhibited Vstat40 processing at a level comparable to equimolar inhibition with dec-RVKR-cmk, while a control inhibitor containing the chloromethylketone group had no effect (Figure 5A). To examine whether the activity of other PCs or metalloproteinases accounts for the majority of the proteolytic cleavage in the absence of furin, we treated BAI1-transfected LoVo cells with equimolar dec-RVKR-cmk and GM6001 singly or in combination (Figure 5B). For both inhibitors, single treatments reduced the levels of secreted Vstat40 in the CM while combined treatment largely abolished Vstat40 processing. These results are compatible with the interpretation that dec-RVKR-cmk inhibits residual

PC activity in LoVo cells, and that these PCs may activate the metalloproteinase processing Vstat40 in the absence of furin as a compensatory mechanism.

To confirm the involvement of metalloproteinases in Vstat40 cleavage, we wished to determine whether tissue inhibitors of metalloproteinases (TIMPs) regulate this processing event. Overexpression of TIMPs 1-3 in 293 cells transiently co-transfected with *BAI1* cDNA showed a clear inhibitory effect of TIMP-3 on Vstat40 processing (Figure 5C). Levels of pro- and active forms of MMP-14, an endogenous TIMP-3 target, were not affected by this manipulation. We conclude that PC and metalloproteinase activities are responsible for Vstat40 processing, either independently or in a sequential fashion.

MMP-14 directly processes extracellular BAI1 into Vstat40

In our search for the metalloproteinase cleaving BAI1, we focused first on MMP-14 for its role in glioma biology and activation of other MMPs (30-32). SiRNA-mediated knockdown of MMP-14 expression yielded virtually complete abrogation of Vstat40 processing by 72 hours post-transfection even in the presence of furin (Figure 6A), suggesting that MMP-14 is essential for Vstat40 generation and acts downstream of furin. As expected, this was accompanied by an accumulation of uncleaved full-length BAI1. Since MMP-14 is known to activate other matrix metalloproteinases, including MMP-2 and MMP-8, we wished to determine whether Vstat40 processing was directly mediated by MMP-14 or involved its target MMPs. Treatment of BAI1-transfected 293 cells with specific inhibitors of MMP-3, MMP-2/9, and MMP-8 did not yield a substantial inhibition of Vstat40 processing (Figure 6B).

To verify that MMP-14 is the enzyme cleaving Vstat40, we performed an *in vitro* cleavage experiment, incubating the recombinant active catalytic domain of human MMP-14 with CM containing Vstat120 (Figure 6C). After 1.5 and 18.5 hours of incubation, Vstat120 levels decreased strongly and Vstat40 levels showed a corresponding increase. We conclude that MMP-14 is sufficient to process Vstat40 from BAI1 and is likely a mediator of this process in culture and *in vivo*, as we observed that pro and active forms of MMP-14 are abundantly expressed in normal brain tissue in addition to the Vstat40 fragment (Figure 6D). While MMP cleavage sites are less well defined compared with furin cleavage sites, *in vitro* studies have demonstrated that the position of certain amino acids mediates efficiency of MMP-14 proteolytic activity (33). In this work, MMP-14 is found to prefer a P1-P1’-P2’ motif of Ser-Leu-Arg, where P1 indicates the amino acid directly N-terminal to the cleavage and P1’ is the amino acid directly C-terminal to the cleavage. Based on these studies, we predict that MMP-14 cleaves BAI1 into Vstat40 between Ser_{326} and Leu_{327} (see open triangle in Fig. 3C), although this assertion will need to be formally demonstrated biochemically in a future study using sequencing or mass spectrometry of the cleavage products.

Discussion

BAI1 has been identified as an important tumor suppressor mutated (9) or lost (10) in cancer, yet little is known about its bioactivity or regulation. The present work represents a significant advance as we demonstrate that the N-terminus of BAI1 is proteolytically

processed into an abundant 40 kDa fragment named Vstat40, which unexpectedly shows potent anti-angiogenic activity *in vitro* and *in vivo*.

We demonstrate that BAI1 is unique amongst the class B GPCRs for it's shedding of cryptic angioinhibins and that the release of Vstat40 and Vstat120 occurs by different and exclusive mechanisms, suggesting complex multi-level regulation. The processing of Vstat40 occurs extracellularly and is mediated by the membrane-bound matrix metalloprotease 14 (MMP-14, also known as MT-MMP1), an enzyme, which depends upon the activity of proprotein convertases (PCs) in the trans-Golgi network to be converted to its active form. Our data support a role for furin – and possibly other PCs when furin is silenced – in the activation of BAI1 cleavage by MMP14. BAI1 processing by MMP-14 is very efficient as we show that Vstat40 is the primary secreted fragment in cultured cells and is abundant in normal human brain tissue. This proteolysis is expected to require association of extracellular BAI1 with the cell surface, as secreted Vstat120 was a poor substrate for Vstat40 processing, suggesting that BAI1 and MMP-14 may be colocalized on the cell membrane. Membrane association *per se* may not be sufficient for the cleavage, as we showed that a construct expressing the N-terminus with only three transmembrane anchors is not cleaved very efficiently, supporting a potential role for the full transmembrane region and/or the C-terminus. The consequence of this cleavage is the release of a freely diffusible 40 kDa fragment that can exert angio-regulatory functions on neighboring endothelium. The function of the remnant N-terminal truncated BAI1 remains to be determined.

In contrast, processing of Vstat120 occurs independently of Vstat40 generation at an earlier step during intracellular protein maturation. The large N-terminal domains of adhesion GPCRs are processed via an autoproteolytic mechanism at a conserved GPS site proximal to the cell membrane following a nucleophilic attack of a conserved arginine or histidine on a serine (34, 35). We have previously shown that BAI1 is cleaved at the GPS site (21), and predict BAI2 and 3 will be similarly cleaved, although this remains to be experimentally demonstrated. The resulting fragments typically stay cell-associated due to their binding to the transmembrane domain (36). This autoproteolysis is thought to occur in the endoplasmic reticulum as point mutants in the GPS can impair the ability of these proteins to traffic to the Golgi apparatus (37). Further, proteolysis of the GPS may depend on such post-translational modifications as glycosylation (38) or phosphorylation, as we show here that a phosphomimetic substitution in the BAI1 GPS dramatically increases cleavage efficiency. Further, our data suggest Vstat120 proteolysis is a relatively low efficiency event under physiological conditions, as this fragment is barely detectable in normal human brain. Because the association of the cleaved fragment with the transmembrane portion of the receptor can control intracellular signaling in GPCRs, the ratio of BAI1 cleaved at the GPS or MMP-14 sites might represent alternative functional outcomes. Overall, these findings emphasize that the function and regulation of BAI1 depends upon the processing of its N-terminal domain into alternate fragments by very distinct intra- and extracellular processing events.

Unlike BAIs 2 and 3, the BAI1 N-terminus has an extra TSR and an RGD integrin-binding motif and generation of Vstat40 by MMP-14 separates these domains from the parent BAI1 molecule. Thus, there is no homolog fragment generated from BAI2 and 3, suggesting this is

a distinguishing functional feature between the three family members. Unexpectedly, we found that the anti-angiogenic activity of Vstat40 depends upon the CD36 receptor, presumably via binding of its lone TSR. Typically, TSRs that bind CD36 feature a VCTG sequence believed to interact with the CD36 CLESH domain (39), but Vstat40 lacks this motif. Our studies support prior findings that TSR peptides lacking the intact VTCG motif can still inhibit endothelial cell migration (16) and that this motif may not always be essential for the inhibition of tumor angiogenesis (40). Alternatively, while the Vstat40 TSR does not contain the precise VTCG sequence, its similarities to the canonical motif may be sufficient for this interaction (12), or Vstat40 may associate with some other part of CD36. Our results do not preclude a role for RGD by engaging integrins in the activity of Vstat40, but they indicate that the TSR-CD36 interaction is necessary for its angioregulatory activity.

The precise mechanisms driving loss or mutation of the BAI1 tumor suppressor in cancer remain to be established. MMP-14 is highly expressed on the surface of aggressive cancers including gliomas, where it promotes cancer invasion and progression by degrading multiple components of the extracellular matrix and glioma basal lamina (30, 41, 42). Similarly, furin expression is upregulated in many cancers (43, 44). Our findings indicate that furin and MMP14 upregulation, typically seen as oncogenic steps in cancer formation, have the unwanted consequence of generating a potent secreted angioinhibin expected to antagonize tumor growth. It is, therefore, possible that the synthesis of Vstat40 generates selective pressure driving the concomitant mutation or loss of BAI1 expression (45), an interpretation compatible with our finding of reduced survival in glioma patients expressing low levels of BAI1.

In addition to its angioregulatory function, generation of the Vstat40 fragment is very likely to have other wide-ranging physiological implications. Ultimately, it will be important to study the impact of this cleavage on the function of the full-length BAI1 protein in its capacity as a GPCR, cell adhesion molecule, regulator of synaptic function, or mediator of engulfment (12). In sum, in defining a novel proteolytic cascade mediating the generation of the abundant secreted angiogenesis inhibitor Vstat40, this research both represents an important advance in our understanding of the biology of BAI1 and indicates an avenue of great potential for therapeutic development for cancer and other diseases marked by vascular pathology.

Materials and Methods

Cell culture

Indicated human cell lines and human dermal microvascular endothelial cells (HDMECs) and human umbilical vein endothelial cells (HUVECs) were cultured as previously described (1, 46, 47). Conditioned medium (CM) from control LN229-L16 (stably expressing a tet-on vector) and inducible Vstat40-expressing glioma cells (clone LN229-L16-V40 #17) was prepared in serum-free culture medium containing doxycycline (2 μg/mL) and collected after 48 hours, centrifuged and concentrated 30-fold using an Amicon Ultra concentrator (5 kDa MW cut-off) to a final volume of 500 μL and used at 1x in angiogenesis experiments.

Transfection

Transfections were performed with GenePorter as recommended (Genlantis). For the knockdown assays, a mix of furin siRNA (NE Biolabs ShortCut siRNA mix, N2026S) and MMP-14 siRNA (Ambion , ID# s8877) was used.

Generation of truncation constructs

All truncation constructs (indicated by numbers in parentheses in Fig.3A) were generated by PCR using *Bai1* cDNA as a template (11) and cloned into pcDNA3.1D/V5-His (Invitrogen) using the forward primer 5 ’ CACCCTTAAGCTTCGAGCTAGG and the reverse primers (1) 5’ CTATCAGTCCCGCGTGCATTCGCC, (2) 5’ CTATCAGCCGCCCTCCACGCCCGG, (3) 5’ CTATCAGGGGGCTGGGAACCCAAAC, (4) 5’ CTATCACCAGCCCTCGCCGCAGGTG for untagged constructs and (6) 5’ GCTGGTGCGCCCAGCGGG and (7) 5 ’ TGTGGACCGCAGGGACTG for tagged constructs. Constructs containing mutations in RSQ and SLR motifs were generated in full-length BAI1 in pcDNA 3.1. Primer overlap extension using mutagenic primer sequences was used to create inserts containing indicated mutations: SLRfwd: 5 ’ C A GGCAGCAGCATCCACAGATGCCCGGCG; SLRrev: 5 ’ GGATGCTGCTGCCTGGCTCCGGGAGCTGG; RSQfwd: 5’ TCCGCAGCAGCATCCCTGCGGTCCAC A G A T ; RSQrev: 5’ GGATGCTGCTGCGGAGCTGGTGCGCCCAG. Inserts were cloned at two unique sites (XhoI and AgeI) flanking the Vstat40 cleavage site and the presence of the mutation was confirmed by sequencing.

Western blot

Western blots were performed as previously described (23) using the following antibodies and dilutions: BAI1 N-terminal antibody N-Ab (#14933 (1), 1:1000); MMP-14 (ab38971) and TIMP-3 (ab66022) (Abcam, 1:1000); TIMP-1 and -2 (Calbiochem Cat# IM32 and IM11, 1:1000); p53 and actin (Santa Cruz; 1:2500); furin (MON-152 monoclonal antibody; 1:500).

In vitro cleavage reactions

Vstat40-containing CM was collected after 72 hours, filtered and concentrated 60x using Amicon Ultra centrifugal filter devices (5 kDa MW cut-off) to a final volume of 500μL. Concentrates were evenly divided and added to 15 mL of freshly prepared hydrolysis buffers for Furin (1mM $CaCl_2$, 100 mM HEPES, 0.5% Triton X-100, 1 mM β-mercaptoethanol) or MMP-14 (50 mM Tris-HCl, pH 7.5, 150 mM NaCl, 5 mM $CaCl_2$, 0.025% Brij35 detergent), precooled to 4°C. Samples were buffer-exchanged to a final volume of 500 μL each and portioned into input and treatment samples on ice. Input samples were immediately precipitated with four volumes of ice-cold acetone and stored at −20°C. 0.2 μg of the catalytic domain of either furin (New England Biolabs Cat. # 8077S) or MMP14 (Calbiochem Cat. # 475935) were added to their respective treatment samples, and control and enzyme-containing samples were incubated at 37°C for the indicated time intervals, after which all samples were precipitated with acetone for Western blot analysis. Catalytic activity of rhFurin was verified by incubation with the fluorogenic furin substrate peptide

Boc-RVRR-AMC (Alexis Biochemicals, Cat. # ALX-260-040). Fluorescence of the substrate peptide in buffer-exchanged CM either with or without rhFurin (1U/mL) was measured at indicated time points and normalized to the baseline fluorescence of the substrate in furin hydrolysis buffer alone.

Angiogenesis assays

The modified Boyden chamber and scratch wound endothelial migration assays were performed as described (23).

In the matrigel assay, HDMECs and HUVECs were serum-starved overnight, then seeded into 24-well plates at a density of 50,000 cells/well in complete endothelial medium containing 1x control or Vstat-containing CM. Wells were precoated with 250 μL of Matrigel and cells were plated in triplicate for each condition. Vascular structure formation was quantified 24 hr later with three views per well at 10x magnification.

The quantitative directed *in vivo* angiogenesis assay (DIVAA) was performed as recommended (Trevigen, Catalog # 3450-048-K). Briefly, basement membrane extract was thawed and prepared with VEGF (0.5 ng/ μL), bFGF (1.5 ng/μL) and heparin (100 ng/μL). The extract was then divided and mixed with concentrated CM (20 μL CM per 200 μL of extract). Provided “angioreactor” tubes were filled with 20 μL of CM/extract mix, inverted and incubated at 37°C for an hour to promote solidification of the gel and thereafter subcutaneously implanted in anesthetized 9-week old female nude mice (Harlan). After twelve days the tubes were excised, photographed, the gel suspensions removed and incubated in 10% FBS-containing culture medium for 1 hour at 37°C to promote recovery of cell-surface molecules including endothelial cell glycoproteins recognized by lectin. Cells were incubated overnight at 4°C with prepared FITC-lectin solution, washed and fluorescence was quantified using a fluorometer (485 nm excitation, 538 nm emission).

Acknowledgments

Paper contributions. SMC performed Vstat40 characterization, angiogenesis, cleavage site detection and furin/MMP-14 protease identification experiments, and SMC and EGVM wrote the manuscript. NSD, BK, EMS and SK performed Vstat40 and protease identification experiments. LC and JHS performed the survival analysis. Experiments were conceived of and planned by the respective authors under the direction of EGVM.

We appreciate the helpful advice and assistance of all members of the Laboratory of Molecular Neuro-Oncology. SMC was in the Emory graduate program in Neuroscience and acknowledges project guidance by her thesis committee (Drs. Randy Hall, Robert McKeon, Paula Vertino, and Wei Zhou). We thank Dr. C. Dubois (Université de Sherbrooke) for the kind gift of LoVo cells. The US National Institutes of Health (R01 CA86335 to EGVM and contract 29XS193 to JHS), the Emory Neurosciences Initiative and University Research Council (to EGVM) contributed to the funding of this research.

References

1. Kaur B, Brat DJ, Calkins CC, Van Meir EG. Brain angiogenesis inhibitor 1 is differentially expressed in normal brain and glioblastoma independently of p53 expression. Am J Pathol. 2003 Jan; 162(1):19–27. [PubMed: 12507886]
2. Nam DH, Park K, Suh YL, Kim JH. Expression of VEGF and brain specific angiogenesis inhibitor-1 in glioblastoma: prognostic significance. Oncol Rep. 2004 Apr; 11(4):863–9. [PubMed: 15010886]

3. Yoshida Y, Oshika Y, Fukushima Y, Tokunaga T, Hatanaka H, Kijima H, et al. Expression of angiostatic factors in colorectal cancer. Int J Oncol. 1999 Dec; 15(6):1221–5. [PubMed: 10568831]
4. Fukushima Y, Oshika Y, Tsuchida T, Tokunaga T, Hatanaka H, Kijima H, et al. Brain-specific angiogenesis inhibitor 1 expression is inversely correlated with vascularity and distant metastasis of colorectal cancer. Int J Oncol. 1998 Nov; 13(5):967–70. [PubMed: 9772287]
5. Hatanaka H, Oshika Y, Abe Y, Yoshida Y, Hashimoto T, Handa A, et al. Vascularization is decreased in pulmonary adenocarcinoma expressing brain-specific angiogenesis inhibitor 1 (BAI1). Int J Mol Med. 2000 Feb; 5(2):181–3. [PubMed: 10639598]
6. Kudo S, Konda R, Obara W, Kudo D, Tani K, Nakamura Y, et al. Inhibition of tumor growth through suppression of angiogenesis by brain-specific angiogenesis inhibitor 1 gene transfer in murine renal cell carcinoma. Oncol Rep. 2007 Oct; 18(4):785–91. [PubMed: 17786337]
7. Duda DG, Sunamura M, Lozonschi L, Yokoyama T, Yatsuoka T, Motoi F, et al. Overexpression of the p53-inducible brain-specific angiogenesis inhibitor 1 suppresses efficiently tumour angiogenesis. Br J Cancer. 2002 Feb 1; 86(3):490–6. [PubMed: 11875720]
8. Yoon KC, Ahn KY, Lee JH, Chun BJ, Park SW, Seo MS, et al. Lipid-mediated delivery of brain-specific angiogenesis inhibitor 1 gene reduces corneal neovascularization in an in vivo rabbit model. Gene Ther. 2005 Apr; 12(7):617–24. [PubMed: 15703766]
9. Kan Z, Jaiswal BS, Stinson J, Janakiraman V, Bhatt D, Stern HM, et al. Diverse somatic mutation patterns and pathway alterations in human cancers. Nature. 2010 Aug 12; 466(7308):869–73. [PubMed: 20668451]
10. Zhu, D.; Vertino, P.; Van Meir, EG. Overexpression of MBD2 contributes to epigenetic silencing of BAI1 in glioblastoma. 2011.
11. Nishimori H, Shiratsuchi T, Urano T, Kimura Y, Kiyono K, Tatsumi K, et al. A novel brain-specific p53-target gene, BAI1, containing thrombospondin type 1 repeats inhibits experimental angiogenesis. Oncogene. 1997; 15(18):2145–50. [PubMed: 9393972]
12. Cork, SM.; Van Meir, EG. BAIs: novel regulators of signaling and disease. 2011.
13. Van Meir EG, Polverini PJ, Chazin VR, Huang H-JS, de Tribolet N, Cavenee WK. Release of an inhibitor of angiogenesis upon induction of wild type p53 expression in glioblastoma cells. Nature Genet. 1994; 8(2):171–6. [PubMed: 7531056]
14. Zhang X, Lawler J. Thrombospondin-based antiangiogenic therapy. Microvasc Res. 2007 Sep-Nov;74(2–3):90–9. [PubMed: 17559888]
15. Gupta K, Gupta P, Wild R, Ramakrishnan S, Hebbel RP. Binding and displacement of vascular endothelial growth factor (VEGF) by thrombospondin: effect on human microvascular endothelial cell proliferation and angiogenesis. Angiogenesis. 1999; 3(2):147–58. [PubMed: 14517432]
16. Dawson DW, Pearce SF, Zhong R, Silverstein RL, Frazier WA, Bouck NP. CD36 mediates the In vitro inhibitory effects of thrombospondin-1 on endothelial cells. J Cell Biol. 1997; 138(3):707–17. [PubMed: 9245797]
17. Jimenez B, Volpert OV, Crawford SE, Febbraio M, Silverstein RL, Bouck N. Signals leading to apoptosis-dependent inhibition of neovascularization by thrombospondin-1. Nat Med. 2000 Jan; 6(1):41–8. [PubMed: 10613822]
18. de Fraipont F, Nicholson AC, Feige JJ, Van Meir EG. Thrombospondins and tumor angiogenesis. Trends Mol Med. 2001 Sep; 7(9):401–7. [PubMed: 11530335]
19. Nicholson AC, Malik SB, Logsdon JM Jr, Van Meir EG. Functional evolution of ADAMTS genes: evidence from analyses of phylogeny and gene organization. BMC Evol Biol. 2005; 5(1):11. [PubMed: 15693998]
20. Park D, Tosello-Trampont AC, Elliott MR, Lu M, Haney LB, Ma Z, et al. BAI1 is an engulfment receptor for apoptotic cells upstream of the ELMO/Dock180/Rac module. Nature. 2007 Nov 15; 450(7168):430–4. [Research Support, N.I.H., Extramural Research Support, Non-U.S. Gov't]. [PubMed: 17960134]
21. Kaur B, Brat DJ, Devi NS, Van Meir EG. Vasculostatin, a proteolytic fragment of brain angiogenesis inhibitor 1, is an antiangiogenic and antitumorigenic factor. Oncogene. 2005; 24(22): 3632–42. [PubMed: 15782143]

22. Hardcastle J, Kurozumi K, Dmitrieva N, Sayers MP, Ahmad S, Waterman P, et al. Enhanced antitumor efficacy of vasculostatin (Vstat120) expressing oncolytic HSV-1. Mol Ther. 2010 Feb; 18(2):285–94. [PubMed: 19844198]

23. Kaur B, Cork SM, Sandberg EM, Devi NS, Zhang Z, Klenotic PA, et al. Vasculostatin inhibits intracranial glioma growth and negatively regulates in vivo angiogenesis through a CD36-dependent mechanism. Cancer Res. 2009 Feb 1; 69(3):1212–20. [PubMed: 19176395]

24. Guedez L, Rivera AM, Salloum R, Miller ML, Diegmueller JJ, Bungay PM, et al. Quantitative assessment of angiogenic responses by the directed in vivo angiogenesis assay. Am J Pathol. 2003 May; 162(5):1431–9. [PubMed: 12707026]

25. Takahashi S, Nakagawa T, Kasai K, Banno T, Duguay SJ, Van de Ven WJ, et al. A second mutant allele of furin in the processing-incompetent cell line, LoVo. Evidence for involvement of the homo B domain in autocatalytic activation. J Biol Chem. 1995 Nov 3; 270(44):26565–9. [PubMed: 7592877]

26. Sato H, Kinoshita T, Takino T, Nakayama K, Seiki M. Activation of a recombinant membrane type 1-matrix metalloproteinase (MT1-MMP) by furin and its interaction with tissue inhibitor of metalloproteinases (TIMP)-2. FEBS Lett. 1996 Sep 9; 393(1):101–4. [PubMed: 8804434]

27. Cao J, Rehemtulla A, Pavlaki M, Kozarekar P, Chiarelli C. Furin directly cleaves proMMP-2 in the trans-Golgi network resulting in a nonfunctioning proteinase. J Biol Chem. 2005 Mar 25; 280(12): 10974–80. [PubMed: 15637056]

28. Duckert P, Brunak S, Blom N. Prediction of proprotein convertase cleavage sites. Protein Eng Des Sel. 2004 Jan; 17(1):107–12. [Research Support, Non-U.S. Gov't]. [PubMed: 14985543]

29. Thomas G. Furin at the cutting edge: from protein traffic to embryogenesis and disease. Nat Rev Mol Cell Biol. 2002 Oct; 3(10):753–66. [PubMed: 12360192]

30. Fillmore HL, VanMeter TE, Broaddus WC. Membrane-type matrix metalloproteinases (MT-MMPs): expression and function during glioma invasion. J Neurooncol. 2001 Jun; 53(2):187–202. [PubMed: 11716070]

31. Hotary KB, Yana I, Sabeh F, Li XY, Holmbeck K, Birkedal-Hansen H, et al. Matrix metalloproteinases (MMPs) regulate fibrin-invasive activity via MT1-MMP-dependent and -independent processes. J Exp Med. 2002 Feb 4; 195(3):295–308. [PubMed: 11828004]

32. Itoh Y, Takamura A, Ito N, Maru Y, Sato H, Suenaga N, et al. Homophilic complex formation of MT1-MMP facilitates proMMP-2 activation on the cell surface and promotes tumor cell invasion. Embo J. 2001 Sep 3; 20(17):4782–93. [PubMed: 11532942]

33. Turk BE, Huang LL, Piro ET, Cantley LC. Determination of protease cleavage site motifs using mixture-based oriented peptide libraries. Nat Biotechnol. 2001 Jul; 19(7):661–7. [PubMed: 11433279]

34. Bjarnadottir TK, Fredriksson R, Hoglund PJ, Gloriam DE, Lagerstrom MC, Schioth HB. The human and mouse repertoire of the adhesion family of G-protein-coupled receptors. Genomics. 2004 Jul; 84(1):23–33. [PubMed: 15203201]

35. Lin HH, Chang GW, Davies JQ, Stacey M, Harris J, Gordon S. Autocatalytic cleavage of the EMR2 receptor occurs at a conserved G protein-coupled receptor proteolytic site motif. J Biol Chem. 2004 Jul 23; 279(30):31823–32. [PubMed: 15150276]

36. Krasnoperov V, Lu Y, Buryanovsky L, Neubert TA, Ichtchenko K, Petrenko AG. Post-translational proteolytic processing of the calcium-independent receptor of alpha-latrotoxin (CIRL), a natural chimera of the cell adhesion protein and the G protein-coupled receptor. Role of the G protein-coupled receptor proteolysis site (GPS) motif. J Biol Chem. 2002 Nov 29; 277(48): 46518–26. [PubMed: 12270923]

37. Jin Z, Tietjen I, Bu L, Liu-Yesucevitz L, Gaur SK, Walsh CA, et al. Disease-associated mutations affect GPR56 protein trafficking and cell surface expression. Hum Mol Genet. 2007 Aug 15; 16(16):1972–85. [PubMed: 17576745]

38. Hsiao CC, Cheng KF, Chen HY, Chou YH, Stacey M, Chang GW, et al. Site-specific N-glycosylation regulates the GPS auto-proteolysis of CD97. FEBS Lett. 2009 Oct 6; 583(19):3285–90. [PubMed: 19737555]

39. Klenotic PA, Huang P, Palomo J, Kaur B, Van Meir EG, Vogelbaum MA, et al. Histidine-rich glycoprotein modulates the anti-angiogenic effects of vasculostatin. Am J Pathol. 2010 Apr; 176(4):2039–50. [PubMed: 20167858]
40. Yee KO, Streit M, Hawighorst T, Detmar M, Lawler J. Expression of the type-1 repeats of thrombospondin-1 inhibits tumor growth through activation of transforming growth factor-beta. Am J Pathol. 2004 Aug; 165(2):541–52. [PubMed: 15277228]
41. Belkin AM, Akimov SS, Zaritskaya LS, Ratnikov BI, Deryugina EI, Strongin AY. Matrix-dependent proteolysis of surface transglutaminase by membrane-type metalloproteinase regulates cancer cell adhesion and locomotion. J Biol Chem. 2001 May 25; 276(21):18415–22. [PubMed: 11278623]
42. Sato H, Takino T, Okada Y, Cao J, Shinagawa A, Yamamoto E, et al. A matrix metalloproteinase expressed on the surface of invasive tumour cells. Nature. 1994 Jul 7; 370(6484):61–5. [PubMed: 8015608]
43. Bassi DE, Mahloogi H, Al-Saleem L, Lopez De Cicco R, Ridge JA, Klein-Szanto AJ. Elevated furin expression in aggressive human head and neck tumors and tumor cell lines. Mol Carcinog. 2001 Aug; 31(4):224–32. [PubMed: 11536372]
44. Mercapide J, Lopez De Cicco R, Bassi DE, Castresana JS, Thomas G, Klein-Szanto AJ. Inhibition of furin-mediated processing results in suppression of astrocytoma cell growth and invasiveness. Clin Cancer Res. 2002 Jun; 8(6):1740–6. [PubMed: 12060611]
45. Zhu D, Hunter SB, Vertino PM, Van Meir EG. Overexpression of MBD2 in glioblastoma maintains epigenetic silencing and inhibits the antiangiogenic function of the tumor suppressor gene BAI1. Cancer Research. 2011 Sep 1; 71(17):5859–70. [Research Support, N.I.H., Extramural Research Support, Non-U.S. Gov't]. [PubMed: 21724586]
46. Ishii N, Maier D, Merlo A, Tada M, Sawamura Y, Diserens AC, et al. Frequent co-alterations of TP53, p16/CDKN2A, p14ARF, PTEN tumor suppressor genes in human glioma cell lines. Brain Pathol. 1999 Jul; 9(3):469–79. [PubMed: 10416987]
47. Beck-Sickinger AG, Grouzmann E, Hoffmann E, Gaida W, van Meir EG, Waeber B, et al. A novel cyclic analog of neuropeptide Y specific for the Y2 receptor. Eur J Biochem. 1992 Jun 15; 206(3): 957–64. [PubMed: 1318842]
48. Takahashi S, Nakagawa T, Kasai K, Banno T, Duguay SJ, Van de Ven WJ, et al. A second mutant allele of furin in the processing-incompetent cell line, LoVo. Evidence for involvement of the homo B domain in autocatalytic activation. The Journal of biological chemistry. 1995 Nov 3; 270(44):26565–9. [Comparative Study Research Support, Non-U.S. Gov't]. [PubMed: 7592877]

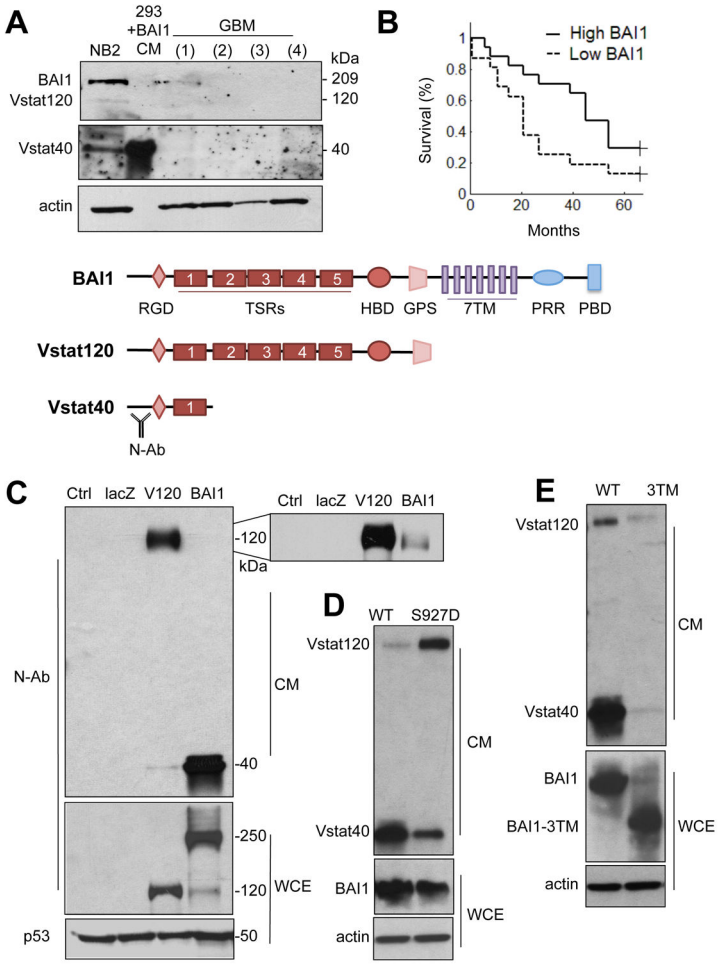

Figure 1. Extracellular BAI1 is processed into two secreted fragments, Vstat120 and the 40 kDa fragment (Vstat40)

(**A**) Upper panel: Western blot showing expression of full-length BAI1 and extracellular derivatives (Vstat40 and Vstat120) in normal human brain cortex (NB2, Emory Brain Tumor bank sample #95-308) and in four randomly-selected specimens of glioblastoma multiforme (GBM; #06-23, #06-19, #05-64, and #05-96, respectively) probed with an N-terminal anti-BAI1 antibody (N-Ab). CM from 293 cells expressing BAI1 was used as a positive control. Lower panel: schematic of BAI1 indicating sizes and features of the Vasculostatins, and the region of the molecule recognized by the N-Ab.

(**B**) *BAI1* mRNA expression data in astrocytoma were obtained from the REMBRANDT database (https://caintegrator.nci.nih.gov/rembrandt/), and samples were divided into low (below-median) and high (above-median) *BAI1* expressors. *BAI1* expression in samples was correlated with respective patient survival data using Kaplan-Meier statistical analysis (p=0.034).

(**C**) Secreted (CM) and intracellular (WCE) BAI1-derived fragments detected with N-Ab in 293 cells 24 hours after transfection with plasmids expressing BAI1, Vstat120 alone, or a control vector (lacZ). UT: untransfected control. Inset shows low levels of Vstat120 are detected in lane 4 upon longer exposure.

(**D**) Levels of secreted 120 and 40 kDa fragments expressing wild type or Ser927Asp ($S_{927}D$)-mutant BAI1. (**E**) Levels of secreted 120 and 40 kDa fragments expressing wild-type BAI1 or BAI1 expressing the extracellular domain and 3 transmembrane repeats (BAI1-3TM).

Abbreviations: RGD: Arginine(Arg)- Glycine(Gly)- Aspartate(Asp); TSR: thrombospondin type-1 repeat; HBD: hormone-binding domain; GPS: GPCR processing site; 7TM: seven-transmembrane region; PRR: proline-rich region; PBD: PDZ-binding domain. N-Ab: BAI1 N-terminal antibody.

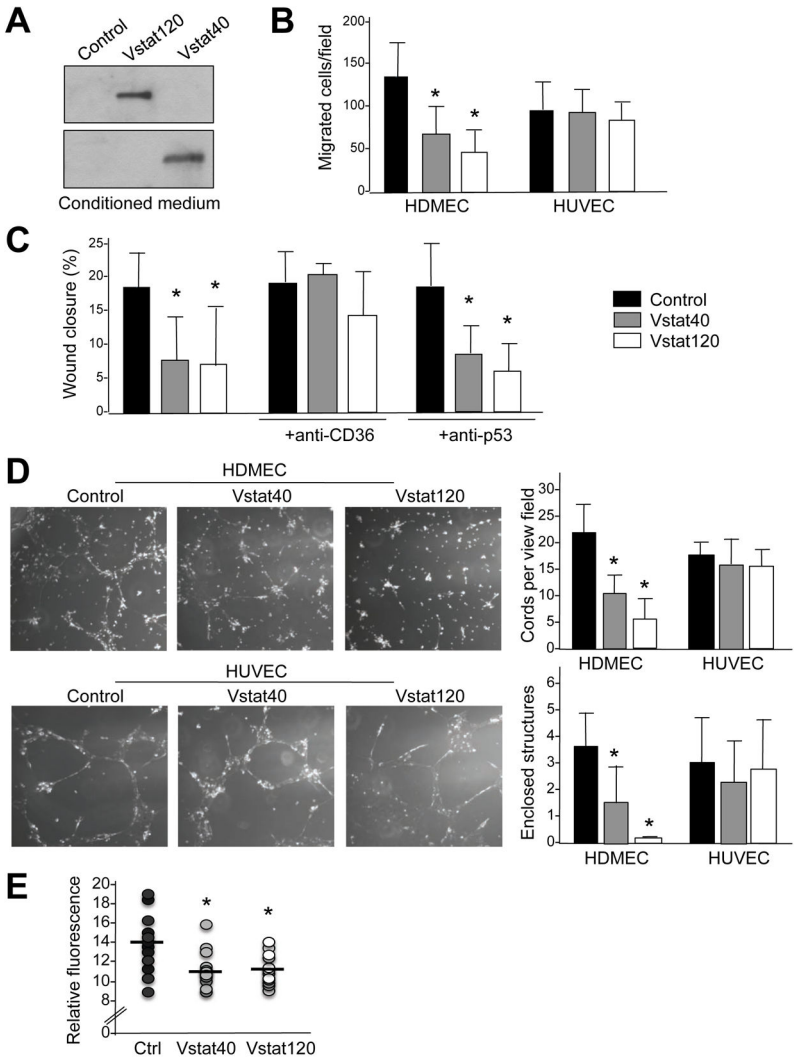

Figure 2. Vstat40 is anti-angiogenic in culture and *in vivo*

(**A**) Representative Western blot of concentrated CM demonstrating expression of Vstat40 in concentrated CM, probed with the BNT antibody. CMs prepared from doxycyline-treated parental LN229-L16 glioma cells (control) or LN229-L16 cells stably transfected with inducible Vstat40 or Vstat120 vectors (tet-on system).

(**B**) Boyden chamber migration assay. The relative migration of CD36-expressing HDMECs and CD36-deficient HUVECs in a Boyden chamber assay was quantified by counting stained cells per view field (Diff-Quik) following 10hrs of incubation with control CM, Vstat40 or Vstat120-containing CM.

(**C**) Endothelial migration scratch wound assay. The ability of an HDMEC monolayer to close a scratch wound after 8 hours was measured in the presence of control or 1x Vstat-containing CM. The role of CD36 was tested by pretreating HDMEC scratches with anti-human CD36 function- blocking antibody (clone FA6-152; 10 μg/mL) or an isotypic control antibody (p53; 10 μg/mL) for 30 minutes prior to incubation with control or Vstat-containing CM.

(**D**) *In vitro* vascular tube formation assay. The formation of endothelial cords and enclosed tube-like structures by HDMECs or HUVECs plated in matrigel with either control CM or CM containing Vstat40 or Vstat120 was quantified.
(**E**) Quantitative directed *in vivo* angiogenesis assay (DIVAA). Angioreactors containing control CM, Vstat40 or Vstat120 CM were implanted subcutaneously in *nu/nu* mice and excised twelve days after implantation. The graph shows the fluorescence of cell pellets derived from angioreactors and stained with FITC-lectin, *Griffonia simplicifolia* (Bandeiraea) isolectin B4 (IB4), which recognizes terminal α-galactosyl residues on endothelial glycoproteins. Graphed data derive from two independent experiments. Significance using Student's t-test was determined using statistical software. Error bars indicate standard deviation from the mean. * = $p < 0.05$.

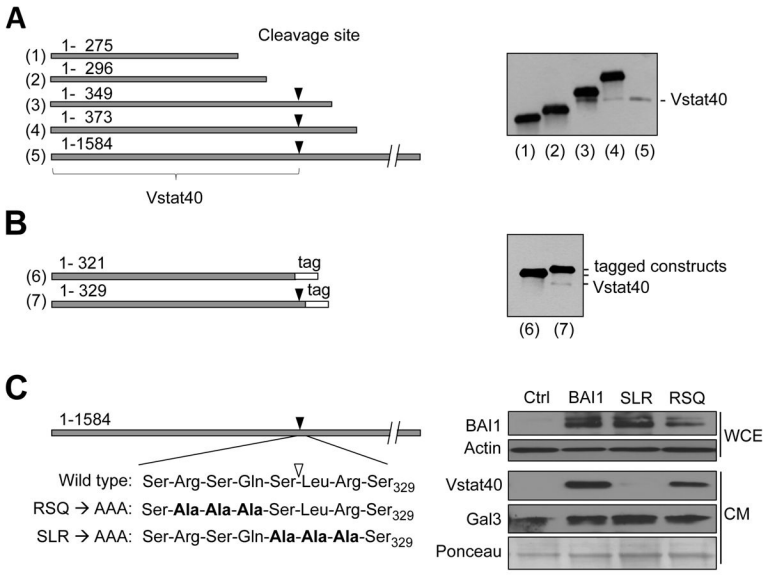

Figure 3. Identification of the site of Vstat40 processing in extracellular BAI1

(**A**) Truncated constructs (1-4) of N-terminal *BAI1* cDNA encompassing the indicated amino acids were transfected into 293 cells and the resulting CM harvested after 48 hours for Western blot analysis with N-Ab. CM from cells transfected with *BAI1* cDNA was used as a marker for Vstat40 size (5). The cleavage site is indicated by a black triangle.

(**B**) Additional truncation constructs (6,7) differing from each other by a few amino acids and expressing a 3-kDa V5/His tag were generated and analyzed to narrow down the localization of the Vstat40 processing site.

(**C**) An alanine mutation approach in full length BAI1 constructs was used to identify the relative contribution of selected amino acids to Vstat40 cleavage. Transient transfection of LN229 cells with BAI1 expression vectors harboring $SLR_{328}\rightarrow AAA$ and $RSQ_{325}\rightarrow AAA$ mutations showed that amino acids SLR are required for Vstat40 processing in the CM (48hrs). Actin was used as a loading control for whole cell extracts (WCE), while Galectin 3 (Gal3) and a Ponceau stain were used to verify equal protein loading in the CM. The putative cleavage site is between amino acids Ser_{326} and Leu_{327} (open triangle, see below).

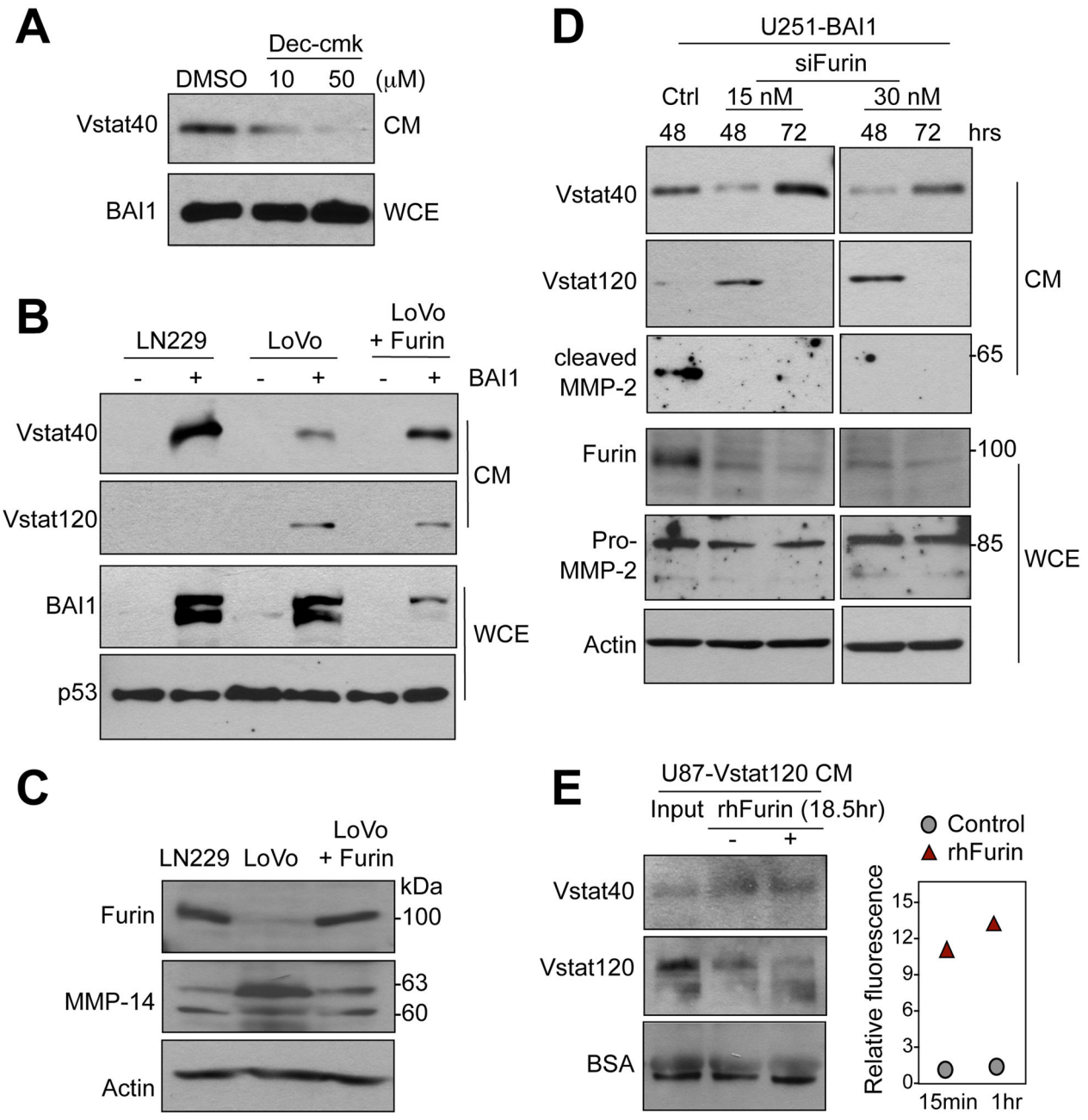

Figure 4. Proprotein convertase activity indirectly regulates Vstat40 processing

(**A**) Western blot showing the dose-dependent inhibition of Vstat40 secretion with dec-RVKR-cmk (Dec-cmk) in the CM of U251MG human glioblastoma cells stably expressing BAI1 (U251-BAI1, clone B12)(23).

(**B**) Levels of Vstat40 and Vstat120 in the CM of control LN229 glioma cells, furin-deficient LoVo cells, and LoVo cells stably transfected with wild-type furin cDNA in the presence (+) or absence (−) of transient transfection with a BAI1 expression vector.

(**C**) Western blot showing the levels of furin and pro (63 kDa) and active (60 kDa) MMP-14 expression in the WCE of LN229 and LoVo cells. Note that the faint furin band in parental

LoVo cells (lane 2) likely originates from the expression of an unstable misfolded mutant furin (48).

(**D**) Levels of Vstats observed in the CM of U251-BAI1 cells after indicated time points following transfection of anti-furin siRNA at a concentration of either 15 or 30 nM. Note that furin levels are strongly downregulated at 48 and 72 hours post-transfection. Levels of secreted cleaved MMP-2 and cellular MMP-2 are used as a control for furin activity.

(**E**) *In vitro* cleavage assay of Vstat120 with rhFurin. (Left) Western blot with N-Ab was used for detection of peptides processed from Vstat120 by recombinant human furin. Concentrated and buffer-exchanged CM from U87MG cells stably transfected with Vstat120 (U87MG-Vstat120) cells was treated with catalytically active rhfurin for 18.5 hours at 37 °C. (Right) To verify the activity of the rhFurin in the CM-buffer solution, the fluorogenic furin substrate was added to the solution −/+ furin and the levels of fluorescence from the cleaved peptide examined.

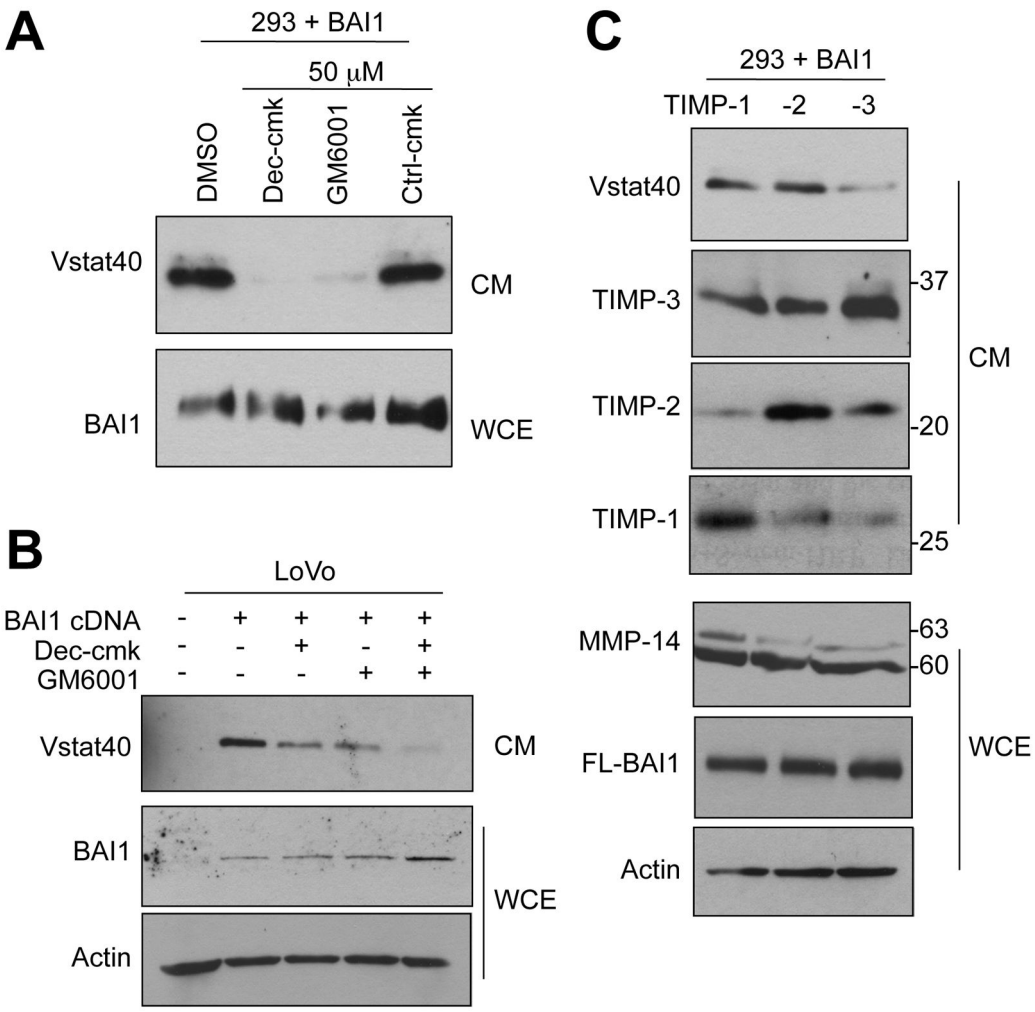

Figure 5. Vstat40 is processed from extracellular BAI1 by a furin-activated metalloproteinase

(**A**) Levels of secreted Vstat40 in the CM of U251-B12 cells after 12 hours incubation with equimolar (50 μM) dec-RVKR-cmk (Dec-cmk; Calbiochem) and the general metalloproteinase inhibitor GM6001 (Calbiochem) compared with equivalent DMSO vehicle treatment. Caspase inhibitor II cmk (Anaspec) was used as a negative control (Ctrl-cmk).

(**B**) Expression of Vstat40 in the CM of LoVo cells transiently transfected with *BAI1* cDNA and treated with dec-RVKR-cmk and GM6001 (50 μM each) as indicated. All conditions received equal amounts of DMSO.

(**C**) Overexpression of tissue inhibitors of metalloproteinases (TIMPs) 1–3 by transient transfection in BAI1-transfected 293 cells implicates TIMP-3 in the inhibition of Vstat40 processing.

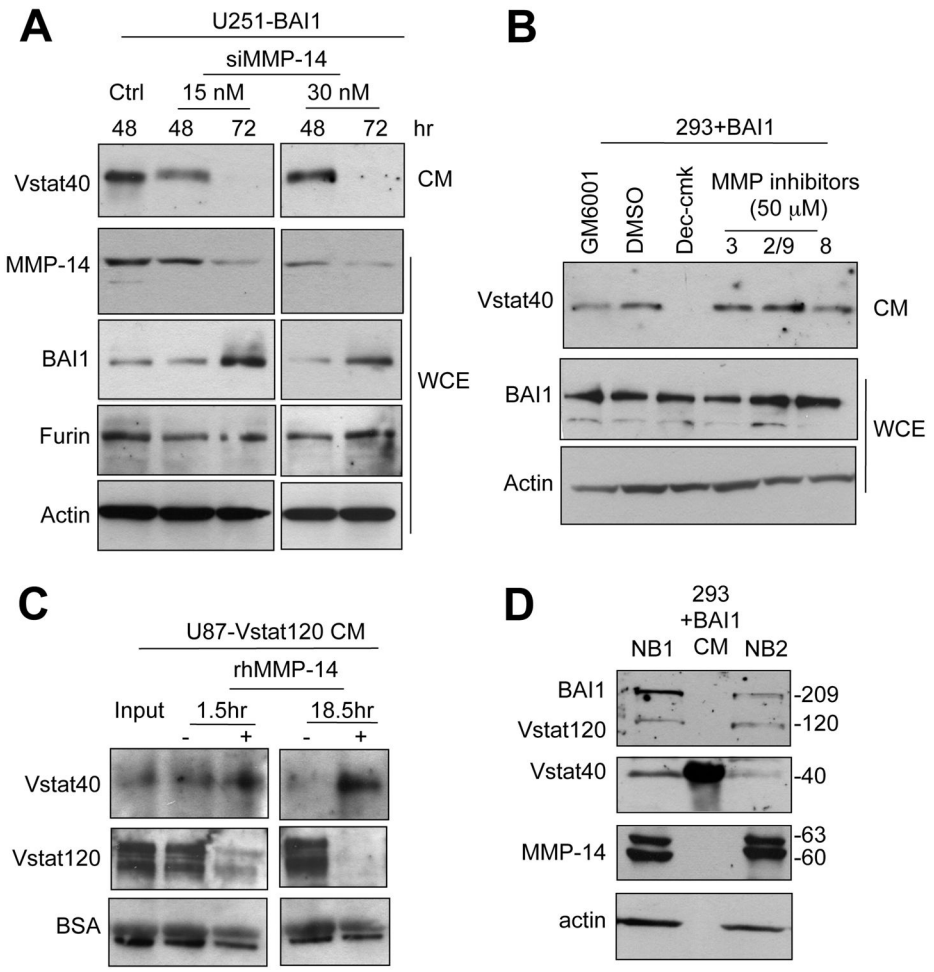

Figure 6. MMP-14 processes BAI1 into Vstat40

(**A**) Evaluation of secreted Vstat40 and cellular BAI1 levels in response to treatment of U251-BAI1 cells with siRNA against MMP-14 at indicated concentrations, for indicated time intervals.

(**B**) Levels of Vstat40 following treatment of U251-BAI1 cells with specific protease inhibitors against MMP-3, MMP-8 or MMP-2/9 (50 μM).

(**C**) *In vitro* cleavage assay of Vstat120 with rhMMP-14. Concentrated CM of U87MG-Vstat120 cells was buffer-exchanged and incubated with recombinant human MMP-14 (rhMMP-14) at 37°C for 1.5 and 18.5 hours. Western blot with the N-Ab evidences the relative levels of Vstat40 and 120 peptides following incubation. Note the decrease of Vstat120 levels and the concomitant increase of Vstat40 with rhMMP-14 treatment.

(**D**) Western blot demonstrating expression of BAI1, Vstat120 and Vstat40 along with pro- (63 kDa) and active MMP-14 (60 kDa) in two independent samples of human non-tumor cortical brain tissue (NB1) (#95-268), and NB2 (#95-308) with CM of BAI1-transfected 293 cells used as a positive control for Vstat40 expression.